Earlier Snowmelt May Lead to Late Season Declines in Plant Productivity and Carbon Sequestration in Arctic Tundra Ecosystems

Donatella Zona (✉ dzona@sdsu.edu)
San Diego State University

Peter Lafleur
Trent University

Koen Hufkens
UMR 1391 ISPA, INRA, 71 avenue Edouard Bourlaux, 33140, Villenave D'Ornon, France

Barbara Bailey
San Diego State University

Beniamino Gioli
National Research Council

George Burba
Licor Environmental

Jordan Goodrich
University of Waikato

Anna Liljedahl
Woodwell Climate Research Center, Falmouth, MA 02540, USA

Eugenie Euskirchen
University of Alaska Fairbanks

Jennifer Watts
Woodwell Climate Research Center, Falmouth, MA 02540, USA

Mary Farina
Woodwell Climate Research Center, Falmouth, MA 02540, USA

John Kimball
University of Montana

Martin Heimann
Max Planck Institute for Biogeochemistry

Mathias Goeckede
Max Planck Institute for Biogeochemistry

Martijn Pallandt
Max Planck Institute for Biogeochemistry

Torben Christensen

Aarhus University

Mikhail Mastepanov

Aarhus University

Efren Lopez-Blanco

Aarhus University

Marcin Jackowicz-Korczynski

Aarhus University

Albertus J. Dolman

VU Amsterdam

Luca Belelli Marchesini

Fondazione Edmund Mach

Roisin Commane

Columbia University

Steve Wofsy

Harvard University

Charles Miller

Jet Propulsion Lab

David Lipson

San Diego State University

Josh Hashemi

San Diego State University

Kyle Arndt

University of New Hampshire

Lars Kutzbach

Universität Hamburg

David Holl

Universität Hamburg

Julia Boike

Humboldt-Universität zu Berlin

Christian Wille

Helmholtz Centre Potsdam - GFZ German Research Centre for Geosciences

Torsten Sachs

Helmholtz Centre Potsdam - GFZ German Research Centre for Geosciences

Aram Kalhori

Helmholtz Centre Potsdam - GFZ German Research Centre for Geosciences

Xia Song

San Diego State University

Xiaofeng Xu

San Diego State University

Elyn Humphreys
  Carleton University

Charles Koven
  Lawrence Berkeley National Laboratory

Oliver Sonnentag
  University of Montreal

Gesa Meyer
  University of Montreal

Gabriel Gosselin
  University of Montreal

Philip Marsh
  University of Waterloo

Walter Oechel
  San Diego State University

Research Article

Earlier snowmelt may lead to late season declines in plant productivity and carbon sequestration in Arctic tundra ecosystems

Donatella Zona[1,2,*], Peter M. Lafleur[3], Koen Hufkens[4,5], Barbara Bailey[1],

Beniamino Gioli[6], George Burba[7,8], Jordan P. Goodrich[9], Anna K. Liljedahl[10,11], Eugénie

S. Euskirchen[12], Jennifer D. Watts[11,13], Mary Farina[11], John S. Kimball[13], Martin

Heimann[14,15], Mathias Göckede[14], Martijn Pallandt[14], Torben R. Christensen[16,17], Mikhail

Mastepanov[16,17], Efrén López-Blanco[16,18], Marcin Jackowicz-Korczynski[16,19], Albertus J.

Dolman[20], Luca Belelli Marchesini[21,22], Roisin Commane[23], Steven C. Wofsy[24], Charles

E. Miller[25], David A. Lipson[1], Josh Hashemi[1], Kyle A. Arndt[26], Lars Kutzbach[27], David

Holl[27], Julia Boike[28,29], Christian Wille[30], Torsten Sachs[30], Aram Kalhori[30], Xia Song[1]

Xiaofeng Xu[1], Elyn R. Humphreys[31], Charles D. Koven[32], Oliver Sonnentag[33], Gesa

Meyer[33], Gabriel H. Gosselin[33], Philip Marsh[34], Walter C. Oechel[1,35]

[1]Department Biology, San Diego State University, San Diego, CA 92182, USA
[2]Department of Animal and Plant Sciences, University of Sheffield, Western Bank,
    Sheffield, S10 2TN, United Kingdom
[3]School of the Environment, Trent University, Peterborough, ON K9L 0G2, Canada
[4]UMR 1391 ISPA, INRA, 71 avenue Edouard Bourlaux, 33140, Villenave D'Ornon,
    France
[5]Department of Applied Ecology and Environmental Biology, Ghent University, 653,
    9000, Ghent, Belgium
[6]IBE, National Research Council (CNR), Institute of BioEconomy, via Giovanni Caproni
    8, Firenze, 50145, Italy
[7]LI-COR Biosciences, 4421 Superior St., Lincoln, NE, 68504, USA
[8]The Robert B. Daugherty Water for Food Global Institute and School of Natural
    Resources, University of Nebraska, Lincoln, NE, 68583
[9]Department of Earth Sciences, University of Waikato, Hillcrest, Hamilton 3216,
New Zealand
[10]Water and Environmental Research Center, University of Alaska Fairbanks, Fairbanks,
    AK 99775-7340, USA
[11]Woodwell Climate Research Center, Falmouth, MA 02540, USA
[12]Institute of Arctic Biology, University of Alaska Fairbanks, Fairbanks, AK, 99775,
    USA

[13]W.A. Franke College of Forestry & Conservation, The University of Montana, Missoula, MT, 59812, USA

[14]Max Planck Institute for Biogeochemistry, 07745 Jena, Germany.

[15]University of Helsinki, Faculty of Science, Institute for Atmospheric and Earth System Research (INAR) / Physics, P.O. Box 64 FI-00014 University of Helsinki, Finland, Gustaf Hällströmin katu 2b, 00560 Helsinki

[16]Department of Bioscience, Arctic Research Centre, Aarhus University, Frederiksborgvej 399, 4000 Roskilde, Denmark

[17]Oulanka Research Station, Oulu University, Kuusamo, Finland

[18]Greenland Institute of Natural Resources, Department of Environment and Minerals, 3900 Nuuk, Greenland

[19]Department of Physical Geography and Ecosystem Science, 22362 Lund University, Lund, Sweden

[20]Department of Earth Sciences, Vrije Universiteit Amsterdam, 1081HV Amsterdam, The Netherlands

[21]Dept. of Sustainable Agro-Ecosystems and Bioresources, Research and Innovation Centre, Fondazione Edmund Mach, via E. Mach 1, 38010 San Michele all'Adige (TN) Italy

[22]Agrarian-Technological Institute, RUDN University, 117198 Moscow, Russia

[23]Dept of Earth and Environmental Sciences, Columbia University, Lamont-Doherty Earth Observatory, Palisades, NY 10964

[24]School of Engineering and Applied Sciences, Harvard University, 20 Oxford St., Cambridge, MA 02138, USA

[25]Jet Propulsion Laboratory, California Institute of Technology, 4800 Oak Grove Drive, Pasadena, CA 91109-8099, USA

[26]Earth Systems Research Center, Institute for the Study of Earth, Oceans, and Space, 8 College Rd, University of New Hampshire, Durham, NH, 03824, United States

[27]Institute of Soil Science, Center for Earth System Research and Sustainability (CEN), Universität Hamburg, 20146 Hamburg, Germany

[28]Geography Department, Humboldt-Universität zu Berlin, 10099 Berlin, Germany

[29]Alfred Wegener Institute Helmholtz Centre for Polar and Marine Research, 14473, Potsdam, Germany

[30]GFZ German Research Centre for Geosciences, 14473 Potsdam, Germany

[31]Department of Geography & Environmental Studies, Carleton University, Ottawa, ON K1S 5B6 Canada

[32]Climate and Ecosystem Sciences Division, Lawrence Berkeley National Laboratory (LBNL), Berkeley, CA 94720, USA

[33]Département de Géographie, Université de Montréal, 1375 Avenue Thérèse-Lavoie-Roux, Montréal, QC H2V 0B3, Canada

[34]Wilfrid Laurier University, Department of Geography and Environmental Studies, 75 University Ave W., Waterloo, ON, Canada, N2S 3C5

[35]Department of Geography, College of Life and Environmental Sciences, University of Exeter, Exeter, EX4 4RJ, UK

*corresponding author email: dzona@sdsu.edu; D.zona@sheffield.ac.uk

79   **Abstract**

80   **Arctic warming is affecting snow cover and soil hydrology, with**

81   **consequences for carbon sequestration in tundra ecosystems. The scarcity of**

82   **observations in the Arctic has limited our understanding of the impact of covarying**

83   **environmental drivers on the carbon balance of tundra ecosystems. In this study, we**

84   **address some of these uncertainties through a novel record of 119 site-years of**

85   **summer data from eddy covariance towers representing dominant tundra**

86   **vegetation types located on continuous permafrost in the Arctic.**

87   **Here we found that earlier snowmelt was associated with more net CO_2**

88   **sequestration and higher gross primary productivity (GPP) only in June and July,**

89   **but with lower net carbon sequestration and lower GPP in August. Although higher**

90   **evapotranspiration (ET) can result in soil drying with the progression of the**

91   **summer, we did not find significantly lower soil moisture with earlier snowmelt, nor**

92   **evidence for a water stress that affected GPP in the peak and late growing season.**

93   **Our results suggest that climate change and the associated increased length in the**

94   **growing season might not benefit these northern tundra ecosystems if they are not**

95   **able to continue sequestering CO_2 later in the season.**

96   **Keywords:** permafrost, carbon loss, climate change, wetlands, snowmelt, plant

97   productivity, senescence

98

99   Climate change is affecting arctic ecosystems through temperature increase

100   (Overland et al., 2019), hydrological changes (Liljedahl et al., 2016), earlier snowmelt

101   (Mudryk et al., 2017; 2019) and the associated increase in growing season length (Piao et

102   al., 2020). Annual arctic air temperature has been increasing at more than double the

103   magnitude of the global mean air temperature increase (Overland et al., 2019), and

104   terrestrial snow cover in June has decreased by 15.2% per decade from 1981–2019

105   (Mudryk et al., 2019). Warming is a main driver of the earlier start of the growing season

106   and of the greening of the Arctic (Lucht et al., 2002; Berner et al., 2020; Myers-Smith et

107   al., 2020). Arctic greening is associated with enhanced vegetation height, biomass, cover

108   and abundance (Forbes et al., 2010). However, the complexity of arctic systems reveals

109   an intricate patchwork of landscape greening and browning (Lara et al., 2018; Miles et

110   al., 2016; Myers-Smith et al., 2020), with browning linked to a variety of stresses to

111   vegetation (Myers-Smith et al., 2020) including water stress (Gonsamo et al., 2019;

112   Gamm et al., 2018). The interconnected changes in temperature, soil moisture, snowmelt

113   timing, etc. can have important effects on the carbon sequestered by arctic ecosystems

114   (Bruhwiler et al., 2021). The reservoir of carbon in arctic soil and vegetation depends on

115   the interaction of two main processes: 1) changes in net CO_2 uptake by vegetation; and 2)

116   increased net loss of CO_2 (from vegetation and soil respiration) to the atmosphere via

117   enhanced respiration. Therefore, defining the response of both plant productivity and

118   ecosystem respiration to environmental changes is needed to predict the response of the

119   net CO_2 fluxes of arctic systems to climate change.

120   An earlier snowmelt, and a longer growing season does not necessarily translate

121   into more carbon sequestered by high latitude ecosystems (Piao et al., 2020). There is

122   large disagreement on the response of plant productivity and of the net CO_2 uptake to

123   early snowmelt in tundra ecosystems (Humphreys and Lafleur, 2011; Parmentier et al.,

124   2011; Lund et al., 2012; Ueyama et al. 2013; López-Blanco et al 2020). A warmer and

125   longer growing season might not result in more net CO_2 uptake if CO_2 loss from

126   respiration increases (Parmentier et al., 2011), particularly later in the season, is more

127   than the CO_2 sequestered by enhanced plant productivity in northern ecosystems (Piao et

128   al., 2008; Parmentier et al., 2011). Moreover, snowmelt timing and the growing season

129   length greatly affect hydrologic conditions of Arctic soils (Liljedahl et al., 2016), as well

130   as plant productivity (Park et al., 2016). Longer non frozen periods earlier in the year

131   (Parida & Buermann, 2014), and earlier vegetation greening can increase

132   evapotranspiration (ET), resulting in lower summer soil moisture (Angert et al., 2005;

133   Buermann et al., 2018; Lian et al., 2020). The complexity in the hydrology of tundra

134   systems comes from the tight link between the water drainage and the presence and depth

135   of permafrost. The presence of permafrost reduces vertical water losses, preventing soil

136   drainage in these northern wetlands during most of the summer despite low precipitation

137   input (Rouse, 2000). Increasing rainfall (Zhang et al., 2013) and increased permafrost

138   degradation can increase soil wetness in continuous permafrost regions (Liljedahl et al.,

139   2016). Further permafrost degradation (e.g. ice-wedge melting) increases hydrologic

140   connectivity leading to increased lateral drainage of the landscape and subsequent soil

141   drying (Liljedahl et al., 2016, Christensen et al., 2020).

142   Given the importance of soil moisture in affecting the carbon balance of arctic

143   ecosystems, and its links with snowmelt timing, in this study we investigated the

144   correlation between summer fluxes of CO_2 (i.e., net ecosystem exchange (NEE), gross

145   primary productivity (GPP) ecosystem respiration (ER)), ET, and environmental drivers

146   such as soil moisture, vapor pressure deficit (VPD) and snowmelt timing, while

147   controlling for the other most important drivers of photosynthesis and respiration (such as

148   solar radiation, and air temperature). We expected earlier snowmelt to be correlated with

149   larger ET, lower soil moisture, and a higher VPD particularly during peak and late

150   season, consistent with drying associated with a longer growing season. The lower soil

151   moisture with earlier snowmelt should result in a negative correlation between snowmelt

152   timing and GPP particularly during the peak and late season (when we expect the most

153   water stress), and in a positive correlation between snowmelt timing and ER during the

154   entire growing season. This soil moisture limitation to plant productivity should result in

155   lower net cumulative CO_2 sequestration during the entire summer (because of lower plant

156   productivity if these ecosystems are water limited due to lower soil moisture with earlier

157   snowmelt). Given that northern ecosystems are considered to be mostly temperature

158   limited, we also tested if warmer conditions were associated with higher productivity and

159   net CO_2 sequestration. We expect that higher temperatures were associated with higher

160   GPP, and ER, but not with higher net CO_2 sequestration if ER increases more than GPP.

161   **Testing the impact of snowmelt timing on the carbon dynamics and**

162   **hydrology of tundra ecosystems.** The 11 sites were selected as among the longest

163   running tower sites in the circumpolar Arctic (including 6 to 19 years of fluxes per site,

164   Table S1). All sites lie in zones of continuous permafrost regions, including a total of 119

165   site-years (summer only: June to August) of eddy covariance CO_2 flux data. These sites

166   are representative of dominant tundra vegetation (wetland, graminoids, and shrub tundra),

167   together accounting for 31% of all tundra vegetation types (Fig. 1, Walker et al., 2005

168   and Supplementary Information). Given the complex interactions among different

169   variables (many covarying together), we used a variety of statistical analyses to identify

170   the association between the standardized anomalies of NEE, GPP, ER, and ET, and the

171   standardized anomalies of main environmental controls during different times of the

172   summer corresponding to various stages in seasonal phenology (early season: June, peak

173   season: July, and late season: August). A partial correlation analysis was used to identify

174   if the timing of the snowmelt associates with anomalies of ET, soil moisture, NEE, GPP,

175   ER, VPD, or the Bowen ratio (the ratio between Sensible Heat (H) and Latent Heat (LE))

176   while considering key meteorological forcing such as air temperature and solar radiation

177   (Methods). Identifying the correlation between ET (and the Bowen ratio) and snowmelt

178   timing is a way to assess water limitation to ecosystems (in addition to testing their

179   response of soil moisture changes), as H and therefore the Bowen ratio are expected to

180   increase with surface drying (Stiegler et al., 2016; Vourlitis and Oechel, 1997). To

181   identify the association between the snowmelt timing, the main environmental variables

182   (i.e., air temperature and solar radiation), and NEE, GPP, ER and ET over time, we

183   performed a maximum covariance analysis (MCA) on the monthly median standardized

184   anomalies from 2004-2019 (a time period when most of the sites had data available)

185   retaining sites as the unit of variation. MCA allowed us to find patterns in two space-time

186   datasets that are highly correlated using a cross-covariance matrix (Lian et al., 2020). The

187   goal of this analysis was to identify the most important environmental drivers associated

188   with NEE, GPP, and ER across all the sites over time. MCA is appropriate for this study

189   as it can handle data with gaps and unequal lengths in the datasets. Finally, to evaluate

190   the water balance at different times of the season, we estimated the difference between

191   Potential Evapotranspiration (PET) and the actual ET, and the difference between

192   precipitation (PPT) and ET for each of the sites, years, and months (e.g. June, July, and

193   August). This study did not attempt to describe the long-term temporal changes in the

194   anomalies of snowmelt and carbon fluxes, given the short data record available for some

195   of the sites (i.e. less than 10 years, Table S1), but focused on understanding the

196   association between environmental variables and the carbon balance at different times of

197   the season. More details of these analyses are included in the Methods.

198

199   **Influence of snowmelt timing on NEE, GPP, ER, and hydrological status of**

200   **tundra ecosystems.** Once taking the variability in solar radiation and air temperature into

201   account (in a partial correlation, Methods), we observed a significant positive relationship

202   between the snowmelt timing anomalies and NEE anomalies (i.e. earlier snowmelt was

203   associated with a higher net CO_2 sequestration) in June and July, but a negative

204   correlation in August (Fig. 2a, Table 1). A similar relationship was found between

205   snowmelt date anomalies and GPP anomalies, with more positive GPP anomalies (i.e.

206   higher plant productivity) with earlier snowmelt in June and July, and more negative GPP

207   anomalies with earlier snowmelt in August (Fig. 2b, Table 1). Earlier snowmelt was

208   associated with significantly higher ER in both June and July, but there was no

209   significant relationship in August (Fig. 2c, Table 1), suggesting that the late season

210   correlation between NEE and snowmelt timing was mostly driven by the negative

211   correlation between GPP and snowmelt in August. The MCA analysis showed that the

212   anomalies in snowmelt timing had the highest squared covariance fraction (SCF) with the

213   monthly median anomalies of GPP, NEE, and ER in June and July, and the lowest in

214   August over the 2004-2019 period (Fig. 3, Fig. S3-5). In late season, other environmental

215   variables had a higher covariance with the GPP, NEE, and ER anomalies than the

216   snowmelt timing, with VPD showing the highest SCF (Fig. 3, Fig. S3-5).

217   This result is consistent with the discrepancy between the observed increase in the

218   maxNDVI over the last four decades, and the time integrated (TI) NDVI which instead

219   has plateaued in the last two decades and even decreased over the last 10 years in several

220   northern arctic ecosystems (Bhatt et al., 2021). TI-NDVI considers the length of the

221   growing season and phenological variations (Tucker and Sellers 1986), and therefore

222   better integrates the vegetation development during the entire growing season. Moisture

223   has been shown to be important for the NDVI trends (Bhatt et al., 2021; Arndt et al.,

224   2019). Given the potential water limitation to summer carbon uptake in northern

225   ecosystems (Gonsamo et al., 2019; Agert et al., 2005; Parida & Buermann, 2014;

226   Buermann et al., 2018), we tested if an earlier snowmelt was associated with a decrease

227   in soil moisture which would affect GPP and NEE. We only observed a significant (and

228   positive) correlation between soil moisture anomalies and snowmelt date anomalies in

229   June (i.e. higher soil moisture with earlier snowmelt, Fig. S1a, Table S2), but no

230   significant correlation in July and August (Fig. S1a, Table S2). The higher soil moisture

231   with earlier snowmelt is consistent with surface inundation after snowmelt (Bowling et

232   al., 2003; Woo et al., 2006) and earlier soil thawing resulting in higher soil moisture (i.e.,

233   soil moisture is low while soils are frozen). A similar result was observed for the ET

234   anomalies: the higher ET with earlier snowmelt in June (Fig. S1b) could be the result of

235   surface inundation after snowmelt (Vourlitis and Oechel, 1997). The standardized NEE

236   anomalies were significantly correlated with the soil moisture anomalies in each of the

237   summer months (Fig. S1d, Table S2). However the relationship between the GPP (and

238   ER anomalies) and soil moisture anomalies was only significant in June (Fig. S1e,f,

239   Table S2) suggesting soil moisture did not affect plant productivity (and respiration) in

240   peak and late season, and the early season positive association might have been mostly

241   driven by an earlier activation of the vegetation with earlier soil thaw (and the associated

242   higher soil moisture). A higher water loss from ET in early season (Fig. S1b) could have

243   resulted in the drying of the surface moss layer with the progression of the summer,

244   which would have been consistent with the observed lower GPP and the lower net CO_2

245   sequestration with earlier snowmelt observed in August (Fig. 2a,b, Table 1). A potential

246   moisture limitation to plant productivity might have been consistent also with the highest

247   SCF of GPP and VPD anomalies in August than in June and July (Fig. S3). However, no

248   significant relationship between ET (or soil moisture) and snowmelt date anomalies was

249   observed in July and August (Fig. S1a,b) contrary to what would be expected if drying

250   occurred following earlier snowmelt. No significant relationship was found between VPD

251   anomalies and snowmelt date anomalies in any of the summer months (P=0.14 in a

252   partial correlation considering air temperature and solar radiation anomalies). Finally,

253   surface drying should result in an increase in the Bowen ratio anomalies with the

254   progression of the summer, given that H increases with a decrease in water table and

255   surface drying (Vourlitis and Oechel, 1997; Goeckede et al., 2017). However, the Bowen

256   ratio showed no correlation with the standardized snowmelt date anomalies in any of the

257   summer months (Fig. S1c, Table S2), and presented similar values in all the summer

258   months (Fig. S2a). Anomalies in GPP and ER anomalies were positively correlated with

259   both air temperature anomalies in all the summer months with no significant difference

260   among the months (Fig. 2e,f). These results suggest that temperature (and not moisture)

261   might still be the main limitation to plant growth in these arctic systems. The lack of

262   correlation between the Bowen ratio and snowmelt date anomalies suggests that an earlier

263   snowmelt did not result in significant surface drying. The median PET-ET, the median

264   PPT-ET for all the years and sites included in this analysis (Fig.S2b,c) was also similar in

265   June and July, and slightly higher in August, as reported by others for Russian arctic

266   tundra (Runkle et al. 2014 and Goeckede et al. 2017). Although these analyses do not

267   consider runoff, which can be significant (Liliendahl, et al., 2017; Lian et al., 2020),

268   overall our results do not suggest that an earlier snowmelt resulted in a water stress

269   (possibly from runoff anomalies) that significantly limited plant productivity in these

270   continuous permafrost ecosystems.

271   The negative correlation between the anomalies in the August GPP and snowmelt

272   timing is consistent with earlier senescence in northern plant species (e.g. *Eriophorum*

273   *vaginatum*, a dominant species across these tundra types) compared to southern species

274   growing in the same location in a common garden experiment (Parker et al., 2017). The

275   phenotypic variation was shown to be persisting for decades (Souther et al., 2014), and

276   ecotypes may be unable to extend the length of their growing season and might not be

277   able to take advantage of a longer growing season (Parker et al., 2017). Several studies

278   showed that once plant growth is initiated after the snowmelt in northern ecosystems, it

279   continues only for a fixed number of days until the occurrence of senescence across

280   several plant functional types (Bjorkman et al., 2015; Rosa et al., 2015; Semenchuk et al.,

281   2016). Therefore, the lower GPP in August with earlier snowmelt might not be linked to

282   water limitation to photosynthesis later in the season, but to an earlier senescence arising

283   from endogenous rhythm of growth and senescence that plant functional types living in

284   these extreme conditions developed over decades. An earlier senescence with an earlier

285   start of the growing season after snowmelt in northern ecosystems is consistent with the

286   earlier spring zero- crossing date and an earlier autumn zero-crossing date of the mean

287   detrended seasonal CO_2 variations at Barrow, AK , USA (NOAA ESRL:

288   https://www.esrl.noaa.gov/gmd/ccgg/obspack/) (Piao et al., 2020) during 2013–2017 than

289   during 1980–1984. The spring and autumn zero-crossing date is the time when the

290   detrended seasonal CO_2 variations intersect the zero line in spring and autumn

291   respectively, and can be used as indicator for the start and end of the net CO_2 uptake by

292   vegetation (Keeling et al., 1996; Piao et al., 2017). On the other hand, NDVI

293   measurements show both an earlier start of the season, and a later end of season from

294   1982-1986 to 2008-2012 (Piao et al., 2020). The disagreement between the detrended

295   seasonal atmospheric CO_2 concentration showing an earlier autumn zero-crossing date,

296   and the NDVI measurements showing a later end of season has been explained by the

297   increase in respiration in the fall (Piao et al., 2008). Similar to studies showing a higher

298   increase in ER than in GPP with warming (Piao et al., 2008: Parmentier et al., 2011) we

299   found that higher temperature, while increasing both GPP and ER, resulted in more net

300   CO_2 sequestration only in June (Fig. 2d). The disagreement between atmospheric CO_2

301   concentration (showing an earlier autumn zero-crossing date), and NDVI (showing a later

302   end of season, Piao et al., 2020) may also be explained by the challenges in using NDVI

303   as a proxy for plant productivity in these arctic systems. NDVI has been shown to have a

304   very variable and non-linear relationship with CO_2 fluxes and plant productivity

305   (Beamish et al., 2020). While some arctic ecosystems showed that NDVI was strongly

306   correlated with GPP (explaining 75% of the variation in GPP, Street et al., 2007), other

307   studies showed that NDVI was either not significantly correlated with GPP and NEE

308   (Zona et al., 2010) or was only able to explain a minor fraction (maximum of 25%) of the

309   variation in NEE and GPP in some of these arctic tundra ecosystems (once accounting for

310   the seasonal variation, La Puma et al., 2007; Olivas et al., 2011).

311   In conclusion, earlier snowmelt was associated with more net CO_2 uptake and

312   higher GPP in early and peak season, but less net CO_2 uptake and lower GPP later in the

313   summer, in arctic tundra ecosystems. We could not find evidence of a water limitation to

314   GPP in the late season. We also found that warmer air temperatures were associated with

315   higher plant productivity and ecosystem respiration, but only with higher net CO_2

316   sequestration in June. Although several hypotheses can be forwarded to explain the link

317   between snowmelt and late-season declines in carbon uptake and in plant productivity,

318   the current literature does not provide a definitive explanation (schematic Fig. 4). Future

319   studies should investigate the potential interaction of different processes explaining the

320   response of the carbon dynamics in the Arctic to warming and an earlier snowmelt, and

321   reconstruct the temporal changes in the carbon balance from these systems. The link

322   between the long-term changes in the CO_2 fluxes and NDVI should be better assessed in

323   tundra ecosystems. It should be identified if higher NDVI is associated with higher net

324   CO_2 uptake. In fact, greening of the Arctic might not necessarily translate into more net

325   CO_2 uptake, as early and peak season carbon gains might be offset by a late season CO_2

326   loss, and respiration might counterbalance the increase in plant productivity. A better

327   understanding of the processes driving these temporal changes is a fundamental step in

328   advancing our prediction of the response of the arctic CO_2 balance to changing climate.

329

Materials and Methods

Site description

A total of 11 eddy covariance flux tower sites across the Arctic were used in this study, where each site had at least six summers of flux data available (SI, Table S1). Ecosystem-scale CO_2 fluxes were estimated using the eddy covariance method (Burba et al., 2008, Burba et al., 2012, Burba et al., 2013). Details pertaining to the sites, data processing, and gap-filling are provided in the SI Appendix, Table S1. All sites are located in continuous permafrost tundra regions. The vegetation in the tower sites, the instruments used to measure fluxes, the average environmental conditions at each site, the datasets used in this study for each site, and the references describing the sites are indicated in SI Appendix, Table S1. As shown in Fig. S2, the Bowen ratio reported for this study showed similar values to what previously reported during the growing season months in the Arctic (from 3.9 in a dry heath to 1.6 in a wet fen in Greenland, Stiegler et al., 2016; 0.83 Goeckede et al., 2017 to 0.20-0.25 in two Siberian Arctic sites, Runkle et al., 2014; and 0.51-1.69 in a moist-tussock tundra in Alaska, Vourlitis and Oechel, 1994).

To estimate the standardized anomalies in the soil moisture we selected the most consistent depths and sensors (the same sensor available for the entire time period in each site, or sensors at the most similar depths in each site and across sites when data from the same sensor was not available due to instrument failure). The number of sensors and the soil depths in each of the sites used for all the analyses were: (CA-DL1: N=2, one in a wet location and one in a dry location (both at -10 cm depth); US-Atq: N=1 (2010-2019) (-10 cm depth); US-Ivo: N=4 at -5 cm depth; US-Bes: N= 2 (2 diagonally inserted at 0-

352   10cm); US-Che: N=2 (-8cm and -16cm depth); RU-Sam: N=5 (at -5, -14, in rims at -5, -

353   12, -15 cm depths in the center of ice-wedge polygons); US-ICt: N=2 (at -2.5 cm depth);

354   GL-ZaH: N=2 (2000-2004 vertical 0-6 cm and from 2005 onward are at two horizontal

355   depths : -5cm, -10 cm); CA-TVC: included one sensor inserted horizontally at -20cm

356   depth. More details on the temporal coverage of the soil moisture data from each site are

357   included in the Supplementary Table S1.

358   The R package 'Evapotranspiration' (Version 1.15, Guo et al., 2016) was used to

359   estimate the daily aggregated Priestley-Taylor potential evaporation (McMahon et al.,

360   2012; Priestley and Taylor, 1972) in each of the study sites, then summed into a monthly

361   total and subtracted by the monthly total actual ET measured with eddy covariance in the

362   respective sites to estimate the PET-ET shown in Fig. S2b. Raster files of monthly

363   precipitation accumulation were acquired for the months of June-August from

364   TerraClimate (Abaatzoglou et al., 2018) over the years 1959-2019. Precipitation data was

365   then extracted from the Eddy Covariance tower coordinates using the terra package

366   (Hijmans 2021) in R (R Core Development Team, 2020) to estimate a monthly total

367   precipitation for June, July, and August for each of the sites included in this study (Tables

368   S1). We did not use the precipitation collected by the meteorological sensors installed in

369   the tower sites given the gaps in the site-level dataset. The other environmental variables

370   used in this study were collected at the towers' sites. The median difference between the

371   total precipitation and the total ET in each site was estimated to evaluate the PPT-ET in

372   each study site during each time of the season (June, July, and August as shown in Fig.

373   S2c). The median was used as it is less affected by outliers.

374

375   *Statistical analysis*

376   *Site-level data*

377   For the analyses performed in this study we separated the data into different times

378   of the season (early season: June, peak season: July, late season: August), given that

379   some of the environmental controls could be very different given the distinct stages of

380   vegetation development. A partial correlation analysis was carried out to identify the

381   correlation between the monthly median standardized anomalies (the ratio between the

382   anomalies and the climatological standard deviation) of NEE, GPP, ER, ET, snow melt

383   date and other environmental variables (most of which covary). The NEE, GPP, ER data

384   used in these analyses were gap-filled using standard methodologies as described in the

385   Supplementary Information. The partial correlations tested the relationships between the

386   standardized snowmelt date anomalies and the monthly median standardized anomalies

387   of NEE, GPP, ER, ET, VPD, and soil moisture, retaining sites as the unit of variation

388   (while controlling for solar radiation and air temperature anomalies, main controls on

389   carbon fluxes). The monthly scale was chosen as a more appropriate temporal scale to

390   identify the importance of the variability in soil moisture on CO_2 fluxes (given that soil

391   moisture does not change much at the hourly and weekly scale at these tundra sites). We

392   also tested if the inclusion of site within a linear mixed model changed the results of

393   correlation analysis between the anomalies. To this purpose, linear mixed effects models

394   (nlme package in R, version R4.0.5, R Developing Team) were used to test the

395   significance of the correlation between the above-mentioned anomalies, by including

396   "site" as categorical random effects to account for pseudo-replication due to the different

397   sites measured in different years. Model performance was evaluated based on the Akaike

16

398   information criterion (AIC) values, on the marginal coefficient of determination

399   (R_m^2 similar to the explanatory power of the linear models) for generalized mixed-effects

400   models as output by the "r.squaredGLMM" function within the "MuMIn" package in R

401   (Nakagawa et al., 2013; Johnson et al., 2014). Given the very similar results between the

402   partial correlation and the linear mixed modelling, we only included the results of the

403   partial correlation and linear regression analyses in Table 1, and Table S2.

404   To maximize the dataset for each analysis we included all available time periods

405   for the variables regressed in Fig. 2, but only selected the 2004-2019 period for the

406   Maximum Covariance Analysis (MCA) analysis to include a time period where most

407   sites had data available. The MCA was performed on two fields (e.g. anomalies in NEE

408   and anomalies in snowmelt timing, see Fig. 3, Figs. S3-5); the columns of the two fields

409   are spatial locations (each site was retained as a unit of variation of this analysis) and

410   rows are temporal measurements. The first pair of singular vectors are the phase-space

411   directions when projected that have the largest possible cross-covariance. The singular

412   vectors describe the patterns in the anomalies that are linearly correlated. We used the

413   time series of the first singular value decomposition (SVD) mode to visualize the parts of

414   the datasets that vary together and report the squared covariance fraction (SCF) with the

415   MCA (Fig. 3, Fig. S3-5). Given the limited length of the dataset we did not discuss the

416   long-term changes in the reported anomalies. However, the MCA allowed us to evaluate

417   the influence of snowmelt timing on the carbon balance over time at different times of the

418   growing season. All analyses were carried out in R version 4.0.5 (R Core Team 2021).

419

420

421

Data Availability

423   The eddy covariance data from RU-Che, RU-Cok, and GL-ZaH (previously

424   named DK-ZaH), CA-DL1, were obtained from the European Fluxes Database

425   (http://www.europe-fluxdata.eu/home), from the Ameriflux Database

426   (http://ameriflux.lbl.gov/), with some updated versions provided directly by the principal

427   investigators of each site (e.g. the data from GL-ZaH are also available on: https://data.g-

428   e-m.dk). The data from US-ICh and US-ICs are stored in the

429   http://aon.iab.uaf.edu/data_access. US-Bes, US-Atq, US-Ivo are stored in the Arctic Data

430   Center (Donatella Zona. 2019. Greenhouse gas flux measurements at the zero curtain,

431   North Slope, Alaska, 2012-2019. Arctic Data Center. doi:10.18739/A2X34MS1B).

432
433
434
435
436
437
438
439
440
441
442
443
444
445
446
447
448
449
450
451
452
453
454
455

456
457
458 **Tables**
459
460 **Table 1** Significance (P) and Pearson's correlation coefficient (r) of the relationships
461 between the indicated monthly median standardized anomalies for June, July, and August
462 retaining site as unit of variation. The anomalies of the indicated variables were regressed
463 with air temperature anomalies in a simple linear regression, and with snow depth
464 anomalies using a partial correlation accounting for the anomalies of solar radiation and
465 air temperature, as shown in Fig. 2. The slopes of the regression between air temperature
466 anomalies and GPP and ER anomalies were not significantly different between the
467 different months but we reported the correlations tested for each month separately. The r
468 value was only included when the P<0.1 (given that for P>0.1 we assumed that r is not
469 different from zero).
470

Regression model	month	P	r
NEE ~ snow melt | Rg & air T	June	<0.001	0.42
	July	0.040	0.21
	August	<0.001	-0.48
GPP ~ snow melt | Rg & air T	June	<0.001	-0.52
	July	0.001	-0.33
	August	0.0074	0.27
ER ~ snow melt | Rg & air T	June	<0.001	-0.38
	July	<0.001	-0.34
	August	0.67	-
NEE ~ air T	June	<0.001	-0.35
	July	0.63	-
	August	0.45	-
GPP ~ air T	June	<0.001	0.47
	July	0.0092	0.27
	August	0.0021	0.31
ER ~ air T	June	<0.001	0.45
	July	<0.001	0.39
	August	<0.001	0.40

471
472
473
474
475
476
477
478
479
480
481
482

483
484
485
486
487 **Figures and figure legends**
488
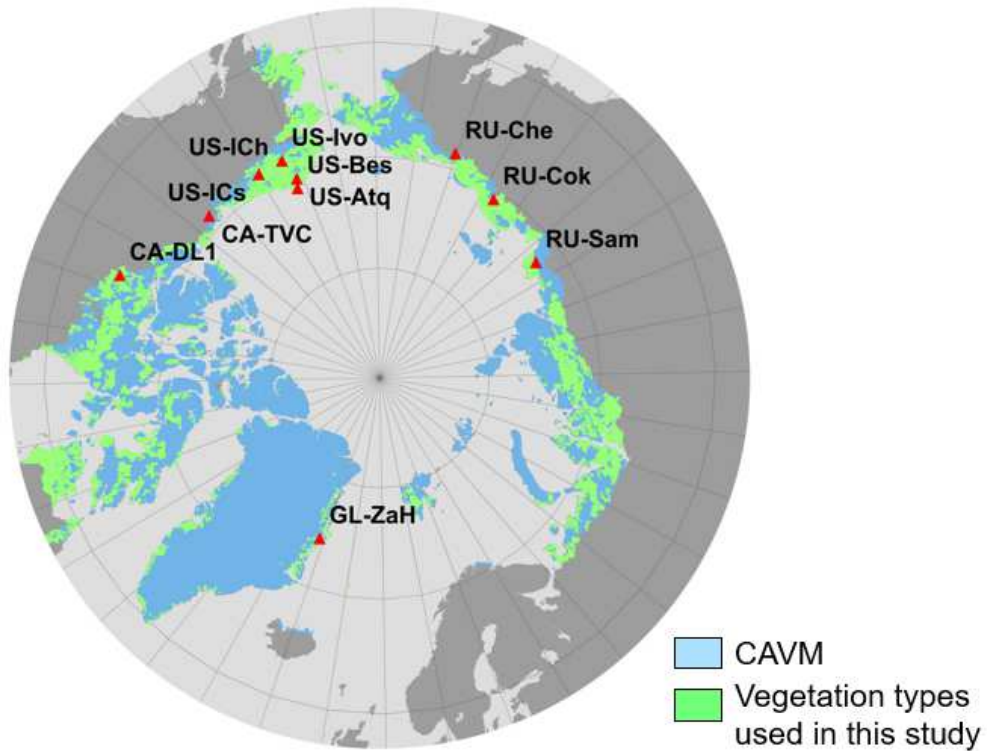
489
490 **Figure 1 | Study sites.** The 11 eddy covariance flux tower sites used in this study. Light
491 blue regions delineate the total Circumpolar Arctic Vegetation Map (CAVM). Green
492 regions delineate the subset of CAVM vegetation types used in this study (including all
493 the vegetation types listed in Table S1).
494
495
496
497
498
499
500
501
502
503
504
505
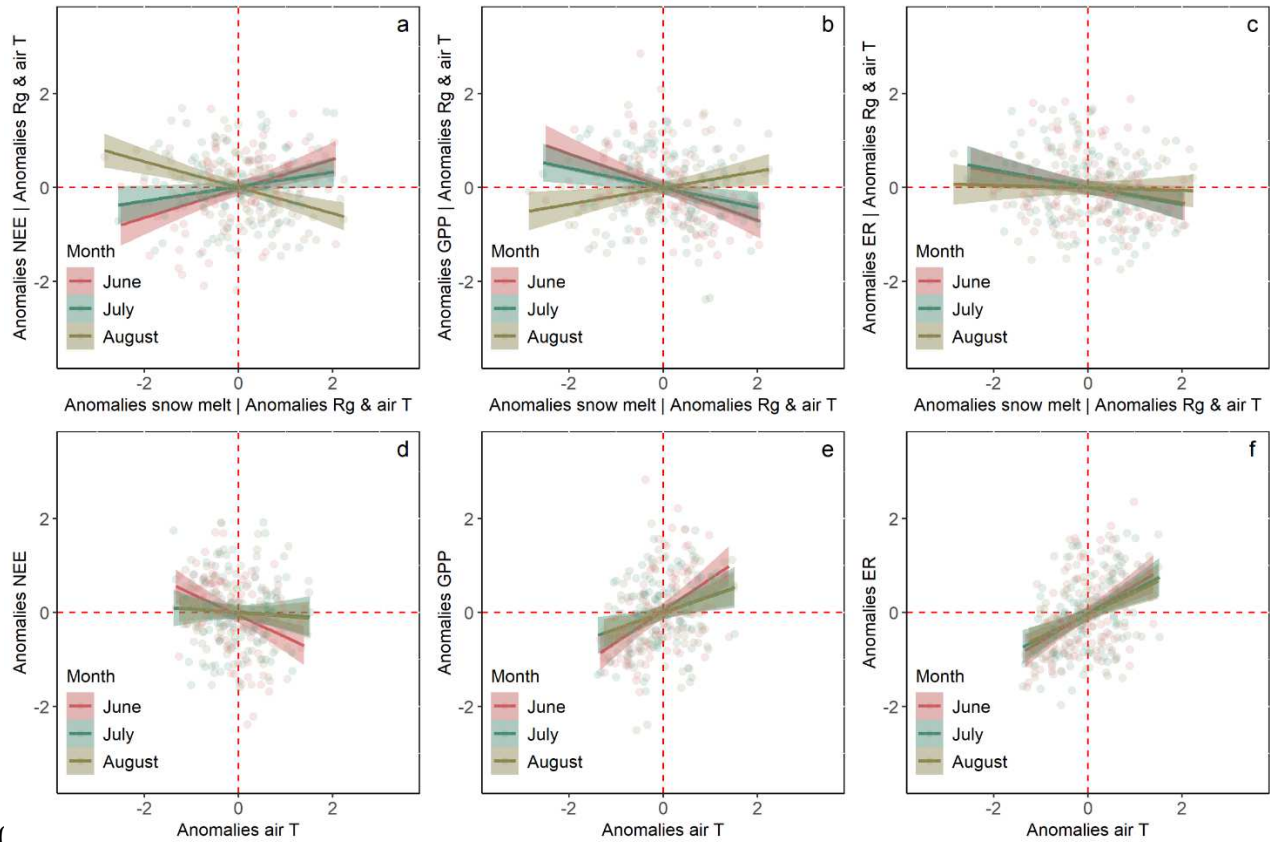
Figure 2 | Relationships between the indicated median monthly anomalies using linear regressions and partial correlation accounting for solar radiation and air temperature anomalies (retaining site as the unit of variation). Given that the interaction term between "month" and snowmelt timing was significant, we included the correlation coefficients and P of the regressions for each of the indicated months in Table 1 (shaded areas are 95% Confidence Intervals). Negative values indicate CO_2 uptake and positive values CO_2 release into the atmosphere.

511
512
513
514
515
516
517
518
519
520
521
522
523
524
525
526
527
528
529
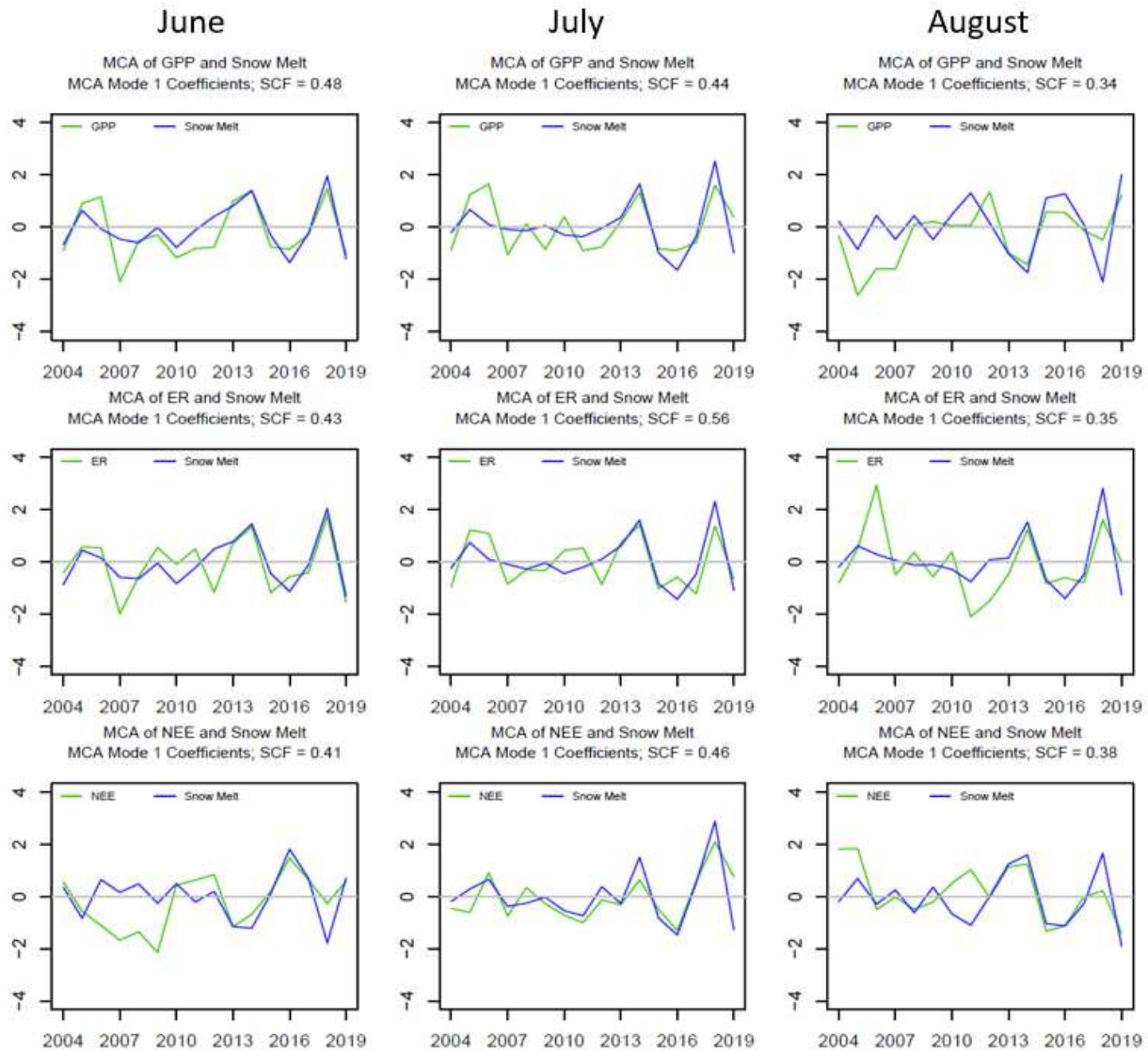
Figure 3 | Maximum covariance analysis (MCA) for the June, July, and August monthly median of the indicated anomalies. The first pair of singular vectors are the phase-space directions when projected that have the largest possible cross-covariance. The singular vectors describe the patterns in the anomalies that are linearly correlated. Displayed is the time series of the first singular value decomposition (SVD) mode which visualizes the parts of the datasets that vary together and included above each panel is the squared covariance fraction (SCF) of each couple of variables. A similar trend and a higher SCF indicates a stronger association over time between the indicated variables.

547
548
549
550
551
552
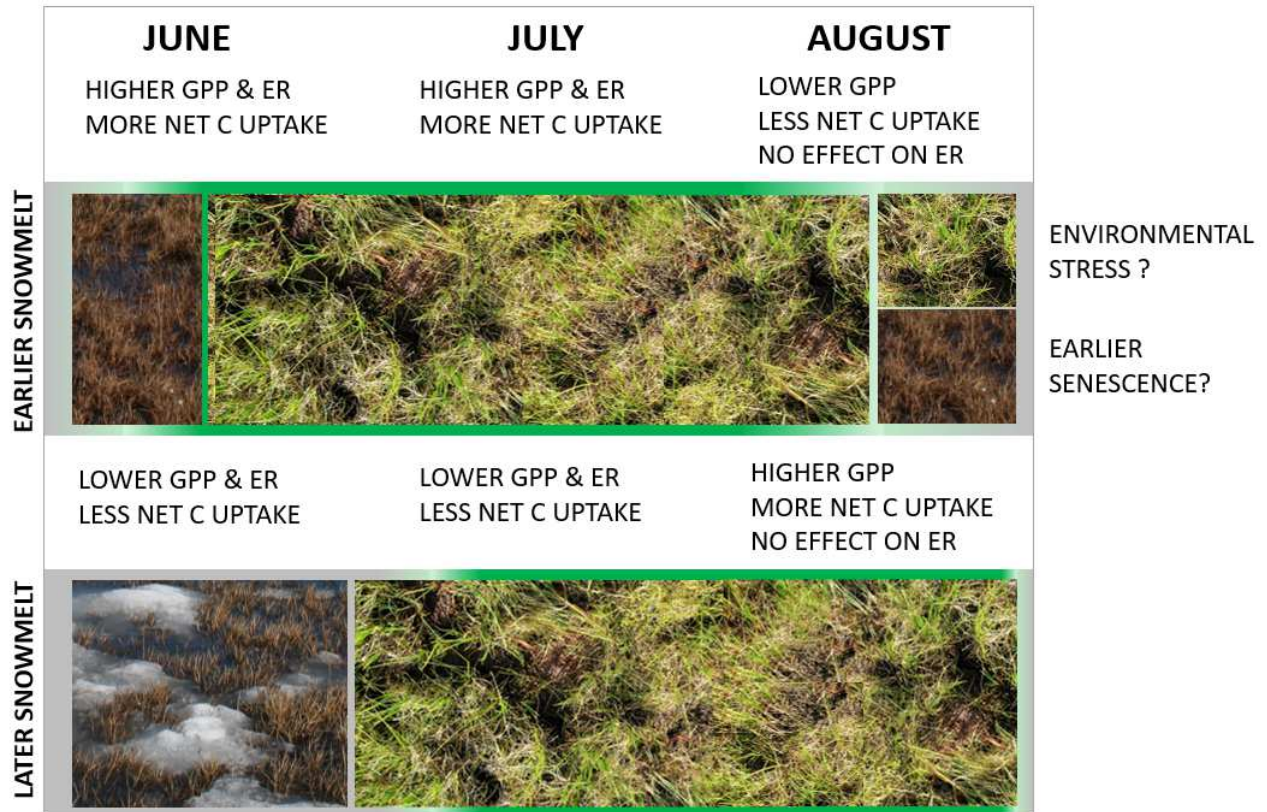
Figure 4 | Schematic of the effect of earlier snowmelt on NEE, GPP, and ER at different times of the season. Earlier snowmelt results in an earlier activation of the vegetation and higher plant productivity and higher net carbon uptake in June and July. This earlier activation could result in a more carbon loss and lower productivity with earlier snowmelt in August, potentially related to either environmental stress or for an earlier senescence.

560

561

562

563

564

587

588

References

590 Abatzoglou JT, Dobrowski SZ, Parks SA, Hegewisch KC. TerraClimate, a high-
591 resolution global dataset of monthly climate and climatic water balance from 1958–2015.
592 Scientific Data 5, 170191 (2018).

593 Angert A, et al. Drier summers cancel out the CO2 uptake enhancement induced by
594 warmer springs. Proceedings of the National Academy of Sciences of the United States of
595 America 102, 10823-10827 (2005).

596 Arndt KA, et al. Arctic greening associated with lengthening growing seasons in
597 Northern Alaska. Environmental Research Letters 14, 125018 (2019).

598 Beamish A, et al. Recent trends and remaining challenges for optical remote sensing of
599 Arctic tundra vegetation: A review and outlook. Remote Sensing of Environment 246,
600 111872 (2020).

601 Berner, L. T. et al. Summer warming explains widespread but not uniform greening in the
602 Arctic tundra biome. Nature Communications 11, 4621, doi:10.1038/s41467-020-18479-
603 5 (2020).

604 Bhatt US, et al. Climate drivers of Arctic tundra variability and change using an
605 indicators framework. Environmental Research Letters 16, 055019 (2021).

606 Boike J, et al. (2019) A 16-year record (2002–2017) of permafrost, active-layer, and
607 meteorological conditions at the Samoylov Island Arctic permafrost research site, Lena
608 River delta, northern Siberia: an opportunity to validate remote-sensing data and land
609 surface, snow, and permafrost models. Earth Syst. Sci. Data 11(1):261-299.

610 Bowling LC, Kane DL, Gieck RE, Hinzman LD, Lettenmaier DP. The role of surface
611 storage in a low-gradient Arctic watershed. Water Resources Research 39, (2003).

612 Bruhwiler, L., Parmentier, F.-J. W., Crill, P., Leonard, M. & Palmer, P. I. The Arctic
613 Carbon Cycle and Its Response to Changing Climate. Current Climate Change Reports 7,
614 14-34, doi:10.1007/s40641-020-00169-5 (2021).

615 Buermann W, et al. Widespread seasonal compensation effects of spring warming on
616 northern plant productivity. Nature 562, 110-114 (2018).

617 Burba G Eddy Covariance Method for Scientific, Industrial, Agricultural and Regulatory
618 Applications: a Field Book on Measuring Ecosystem Gas Exchange and Areal Emission
619 Rates. LI-COR Biosciences, Lincoln, USA, 331 pp. ISBN: 978-0-61576827-4(2013).

620   Burba G, et al. Calculating CO2 and H2O eddy covariance fluxes from an enclosed gas
621   analyzer using an instantaneous mixing ratio. Glob Change Biol 18(1), 385-399 (2012).

622   Burba GG, McDermitt DK, Grelle A, Anderson DJ, & Xu L Addressing the influence of
623   instrument surface heat exchange on the measurements of CO2 flux from open-path gas
624   analyzers. Glob Change Biol 14(8):1854-1876 (2008).

625   Christensen TR, et al. Multiple Ecosystem Effects of Extreme Weather Events in the
626   Arctic. Ecosystems 24, 122-136 (2021).

627   Euskirchen ES, Bret-Harte MS, Shaver GR, Edgar CW, & Romanovsky VE (2017)
628   Long-Term Release of Carbon Dioxide from Arctic Tundra Ecosystems in Alaska.
629   Ecosystems 20(5):960-974.

630   Euskirchen ES, et al. (2006) Importance of recent shifts in soil thermal dynamics on
631   growing season length, productivity, and carbon sequestration in terrestrial high-latitude
632   ecosystems. Glob Change Biol 12(4):731-750.

633   Forbes, B. C., Fauria, M. M. & Zetterberg, P. Russian Arctic warming and 'greening' are
634   closely tracked by tundra shrub willows. Glob. Change Biol. 16, 1542-1554,
635   doi:10.1111/j.1365-2486.2009.02047.x (2010).

636   Gamm, C. M. et al. Declining growth of deciduous shrubs in the warming climate of
637   continental western Greenland. Journal of Ecology 106, 640-654,
638   doi:https://doi.org/10.1111/1365-2745.12882 (2018).

639   Goeckede, M, et al. Shifted energy fluxes, increased Bowen ratios, and reduced thaw
640   depths linked with drainage-induced changes in permafrost ecosystem structure. The
641   Cryosphere 11, 2975-2996 (2017).

642   Gonsamo, A., Ter-Mikaelian, M. T., Chen, J. M. & Chen, J. Does Earlier and Increased
643   Spring Plant Growth Lead to Reduced Summer Soil Moisture and Plant Growth on
644   Landscapes Typical of Tundra-Taiga Interface? Remote Sensing 11, 1989 (2019).

645   Goodrich JP, et al. (2016) Impact of different eddy covariance sensors, site set-up, and
646   maintenance on the annual balance of CO2 and CH4 in the harsh Arctic environment.
647   Agr Forest Meteorol 228-229:239-251.

648   Guo D, Westra S, Maier HR. An R package for modelling actual, potential and reference
649   evapotranspiration. Environmental Modelling & Software 78, 216-224 (2016).

650   Helbig, M. et al. Addressing a systematic bias in carbon dioxide flux measurements with
651   the EC150 and the IRGASON open-path gas analyzers. Agricultural and Forest
652   Meteorology 228-229, 349-359, doi:https://doi.org/10.1016/j.agrformet.2016.07.018
653   (2016).

654   Hijmans RJ terra: Spatial Data Analysis. R package version 1.1-4. https://CRAN.R-
655   project.org/package=terra (2021).

656   Holl D, et al. (2019) A long-term (2002 to 2017) record of closed-path and open-path
657   eddy covariance CO2 net ecosystem exchange fluxes from the Siberian Arctic. Earth
658   Syst. Sci. Data 11(1):221-240.

659   Humphreys ER & Lafleur PM (2011) Does earlier snowmelt lead to greater CO2
660   sequestration in two low Arctic tundra ecosystems? Geophys Res Lett 38(9),
661   doi:10.1029/2011GL047339.

662   Johnson PCD. Extension of Nakagawa & Schielzeth's R2GLMM to random slopes
663   models. Methods in Ecology and Evolution 5, 944-946 (2014).

664   Kade A, Bret-Harte MS, Euskirchen ES, Edgar C, & Fulweber RA (2012) Upscaling of
665   CO2 fluxes from heterogeneous tundra plant communities in Arctic Alaska. J Geophys
666   Res-Biogeo 117(G4).

667   Keeling CD, Chin JFS, Whorf TP. Increased activity of northern vegetation inferred from
668   atmospheric CO2 measurements. Nature 382, 146-149 (1996).

669   Kwon, M. J. et al. Drainage enhances modern soil carbon contribution but reduces old
670   soil carbon contribution to ecosystem respiration in tundra ecosystems. Glob. Change
671   Biol. 25, 1315-1325, doi:10.1111/gcb.14578 (2019).

672   La Puma IP, Philippi TE, Oberbauer SF. Relating NDVI to ecosystem CO2 exchange
673   patterns in response to season length and soil warming manipulations in arctic Alaska.
674   Remote Sensing of Environment 109, 225-236 (2007).
675   https://doi.org/10.1016/j.rse.2007.01.001.

676   Lafleur PM & Humphreys ER (2008) Spring warming and carbon dioxide exchange over
677   low Arctic tundra in central Canada. Glob Change Biol 14: 740–756.

678   Lara, M. J., Nitze, I., Grosse, G., Martin, P. & McGuire, A. D. Reduced arctic tundra
679   productivity linked with landform and climate change interactions. Sci. Rep. 8, 2345
680   (2018).

681   Lian X, et al. Summer soil drying exacerbated by earlier spring greening of northern
682   vegetation. Science Advances 6, eaax0255 (2020).

683   Liljedahl AK, et al. Pan-Arctic ice-wedge degradation in warming permafrost and its
684   influence on tundra hydrology. Nature Geosci 9:312, doi:10.1038/ngeo2674. (2016).

685   Liljedahl AK, Hinzman LD, Kane DL, Oechel WC, Tweedie CE, Zona DE. Tundra water
686   budget and implications of precipitation underestimation. Water Resour Res 53, 6472-
687   6486 (2017).

688   López-Blanco E, et al. Multi-year data-model evaluation reveals the importance of
689   nutrient availability over climate in arctic ecosystem C dynamics. Environmental
690   Research Letters 15, 094007 (2020).

691   Lucht, W. et al. Climatic control of the high- latitude vegetation greening trend and
692   Pinatubo effect. Science. 296, 1687–1689 (2002).

693   Lund M, et al. (2012) Trends in CO2 exchange in a high Arctic tundra heath, 2000–2010.
694   J Geophys Res-Biogeo 117(G2), doi:10.1029/2011jg001901.

695   McMahon TA, Peel MC, Lowe L, Srikanthan R, McVicar TR. Estimating actual,
696   potential, reference crop and pan evaporation using standard meteorological data: a
697   pragmatic synthesis. Hydrol Earth Syst Sci 17, 1331-1363 (2013).

698   Miles, V. V. & Esau, I. Spatial heterogeneity of greening and browning between and
699   within bioclimatic zones in northern West Siberia. Environ. Res. Lett. 11, 115002 (2016).

700   Mudryk L., R. Brown, C. Derksen, K. Luojus, B. Decharme, and S. Helfrich (2019)
701   Terrestrial snow cover, Richter-Menge, J., M. L. Druckenmiller, and M. Jeffries, Eds.:
702   Arctic Report Card 2019, https://www.arctic.noaa.gov/Report-Card.

703   Mudryk LR, Kushner PJ, Derksen C, Thackeray C. Snow cover response to temperature
704   in observational and climate model ensembles. Geophys Res Lett. 2017;44:919–26.
705   https://doi.org/10.1002/2016GL071789.

706   Myers-Smith, I. H. et al. Complexity revealed in the greening of the Arctic. Nature
707   Climate Change 10, 106-117, doi:10.1038/s41558-019-0688-1 (2020).

708   Nakagawa S, Schielzeth H. A general and simple method for obtaining R2 from
709   generalized linear mixed-effects models. Methods in Ecology and Evolution 4, 133-142
710   (2013).

711   Oechel WC, Laskowski CA, Burba G, Gioli B, & Kalhori AAM (2014) Annual patterns
712   and budget of CO2 flux in an Arctic tussock tundra ecosystem. J Geophys Res-Biogeo
713   119(3):323-339, doi:10.1002/2013JG002431.

714   Olivas PC, Oberbauer SF, Tweedie C, Oechel WC, Lin D, Kuchy A. Effects of Fine-
715   Scale Topography on CO2 Flux Components of Alaskan Coastal Plain Tundra: Response
716   to Contrasting Growing Seasons. Arctic, Antarctic, and Alpine Research 43, 256-266
717   (2011).

718   Overland JE, Hanna E, Hanssen-Bauer I, Kim S-J, Walsh JE, Wang M, et al. In: The
719   NOAA Arctic Report Card, Surface Air Temperature 2019,
720   https://arctic.noaa.gov/Report-Card/Report-Card
721   2019/ArtMID/7916/ArticleID/835/Surface-Air-Temperature.

722   Papale, D. & Valentini, R. A new assessment of European forests carbon exchanges by
723   eddy fluxes and artificial neural network spatialization. Glob. Change Biol. 9, 525-535,
724   doi:10.1046/j.1365-2486.2003.00609.x (2003).

725   Parida BR, Buermann W. Increasing summer drying in North American ecosystems in
726   response to longer nonfrozen periods. Geophysical Research Letters 41, 5476-5483

727   (2014).

728   Park T, et al. Changes in growing season duration and productivity of northern vegetation
729   inferred from long-term remote sensing data. Environmental Research Letters 11, 084001
730   (2016).

731   Parker TC, Tang J, Clark MB, Moody MM, Fetcher N. Ecotypic differences in the
732   phenology of the tundra species Eriophorum vaginatum reflect sites of origin. Ecol Evol
733   7, 9775-9786 (2017).

734   Parmentier FJW, et al. Spatial and temporal dynamics in eddy covariance observations of
735   methane fluxes at a tundra site in northeastern Siberia. Journal of Geophysical Research:
736   Biogeosciences 116, G03016 (2011).

737   Piao S, et al. Characteristics, drivers and feedbacks of global greening. Nature Reviews
738   Earth & Environment 1, 14-27 (2020).

739   Piao S, et al. Net carbon dioxide losses of northern ecosystems in response to autumn
740   warming. Nature 451, 49-52 (2008).

741   Piao S, et al. Weakening temperature control on the interannual variations of spring
742   carbon uptake across northern lands. Nature Climate Change 7, 359-363 (2017).

743   Priestley, C & Taylor, R. On the assessment of surface heat flux and evaporation using
744   largescale parameters. Monthly Weather Review, vol. 100, no. 2, pp. 81-92 (1972).

745   R Core Development Team. (2020). R: A language and environment for statistical
746   computing v. 4.0.2. Vienna: R Foundation for Statistical Computing.

747   R Core Team (2019). R: A language and environment for statistical computing. R
748   Foundation for Statistical Computing, Vienna, Austria. URL https://www.R-project.org/.

749   Rosa RK, et al. Plant phenological responses to a long-term experimental extension of
750   growing season and soil warming in the tussock tundra of Alaska. Glob Chang Biol 21,
751   4520-4532 (2015).

752   Rouse, W. R.: The energy and water balance of high-latitude wetlands: controls and
753   extrapolation, Glob. Change Biol., 6, 59–68, 2000.

754   Runkle BRK, Wille C, Gažovič M, Wilmking M, Kutzbach L. The surface energy
755   balance and its drivers in a boreal peatland fen of northwestern Russia. Journal of
756   Hydrology 511, 359-373 (2014).

757   Sachs, T., Giebels, M. , Boike, J. and Kutzbach, L. (2010), Environmental controls on
758   CH4 emission from polygonal tundra on the microsite scale in the Lena river delta,
759   Siberia. Global Change Biology, 16: 3096-3110. doi:10.1111/j.1365-2486.2010.02232.x

760   Semenchuk PR, Gillespie MAK, Rumpf SB, Baggesen N, Elberling B, Cooper EJ. High

Arctic plant phenology is determined by snowmelt patterns but duration of phenological periods is fixed: an example of periodicity. Environmental Research Letters 11, 125006 (2016).

Souther, S, Fetcher, N, Fowler, Z, Shaver, GR, & McGraw, JB Ecotypic differentiation in photosynthesis and growth of Eriophorum vaginatum along a latitudinal gradient in the Arctic tundra. Botany 92, 551-561 (2014).

Stiegler, C., Lund, M., Christensen, T. R., Mastepanov, M., and Lindroth, A.: Two years with extreme and little snowfall: effects on energy partitioning and surface energy exchange in a high-Arctic tundra ecosystem, The Cryosphere, 10, 1395–1413, https://doi.org/10.5194/tc-10-1395-2016, 2016.

Street LE, Shaver GR, Williams M, Van Wijk MT. What is the relationship between changes in canopy leaf area and changes in photosynthetic CO_2 flux in arctic ecosystems? Journal of Ecology 95, 139-150 (2007).

Tucker CJ, Sellers PJ. Satellite remote sensing of primary production. International Journal of Remote Sensing 7, 1395-1416 (1986).

Ueyama M, et al. (2013) Growing season and spatial variations of carbon fluxes of Arctic and boreal ecosystems in Alaska (USA). Ecol Appl 23(8):1798-1816, doi:10.1890/11-0875.1.

Vourlitis GL, Oechel WC. Landscape-Scale CO_2 H_2O Vapour and Energy Flux of Moist-Wet Coastal Tundra Ecosystems over Two Growing Seasons. Journal of Ecology 85, 575-590 (1997).

Walker DA, et al. Phytomass, LAI, and NDVI in northern Alaska: Relationships to summer warmth, soil pH, plant functional types, and extrapolation to the circumpolar Arctic. J Geophys Res-Atmos 108(D2) (2003).

Walker DA, et al. The Circumpolar Arctic vegetation map. Journal of Vegetation Science 16(3):267-282, doi:10.1111/j.1654-1103.2005.tb02365.x (2005).

Walker DA, Gould WA, Maier HA, & Raynolds MK The Circumpolar Arctic Vegetation Map: AVHRR-derived base maps, environmental controls, and integrated mapping procedures. Int J Remote Sens 23(21):4551-4570 (2002).

Woo M-k, Young KL, Brown L. High Arctic Patchy Wetlands: Hydrologic Variability and Their Sustainability. Physical Geography 27, 297-307 (2006).

Zhang X, et al. On the variation of regional CO_2 exchange over temperate and boreal North America. Global Biogeochemical Cycles 27, 2012GB004383 (2013).

Zona D, et al. Cold season emissions dominate the Arctic tundra methane budget. Proc Natl Acad Sci USA 113(1):40-45 (2016).

796 Zona D, Oechel WC, Peterson KM, Clements RJ, Paw U KT, Ustin SL. Characterization
797 of the carbon fluxes of a vegetated drained lake basin chronosequence on the Alaskan
798 Arctic Coastal Plain. Glob Change Biol 16, 1870-1882 (2010).

Supplementary Files

This is a list of supplementary files associated with this preprint. Click to download.

- Supplementaryinformation20211006.pdf